Bioorganic & Medicinal Chemistry Letters 21 (2011) 1176–1180

Contents lists available at ScienceDirect

Bioorganic & Medicinal Chemistry Letters

journal homepage: www.elsevier.com/locate/bmcl

Potent and selective cyclohexyl-derived imidazopyrazine insulin-like growth factor 1 receptor inhibitors with in vivo efficacy

Meizhong Jin [a,*], Andrew Kleinberg [a], Andy Cooke [b], Prafulla C. Gokhale [b], Kenneth Foreman [a], Hanqing Dong [a], Kam W. Siu [a], Mark A. Bittner [b], Kristen M. Mulvihill [a], Yan Yao [a], Darla Landfair [b], Matthew O'Connor [a], Gilda Mak [a], Jonathan A. Pachter [a], Robert Wild [b], Maryland Rosenfeld-Franklin [b], Qunsheng Ji [a], Mark J. Mulvihill [a,*]

[a] (OSI) Oncology, OSI Pharmaceuticals, Inc., 1 Bioscience Park Drive, Farmingdale, NY 11735, United States
[b] (OSI) Oncology, OSI Pharmaceuticals, Inc., 2860 Wilderness Place, Boulder, CO 80301, United States

ARTICLE INFO

Article history:
Received 6 November 2010
Revised 16 December 2010
Accepted 20 December 2010
Available online 23 December 2010

Key words:
Insulin-like growth factor 1 receptor (IGF-1R)
Inhibitors
Tumor growth inhibition (TGI)
Cancer

ABSTRACT

Preclinical and emerging clinical evidence suggests that inhibiting insulin-like growth factor 1 receptor (IGF-1R) signaling may offer a promising therapeutic strategy for the treatment of several types of cancer. This Letter describes the medicinal chemistry effort towards a series of 8-amino-imidazo[1,5-*a*]pyrazine derived inhibitors of IGF-1R which features a substituted quinoline moiety at the C1 position and a cyclohexyl linking moiety at the C3 position. Lead optimization efforts which included the optimization of structure–activity relationships and drug metabolism and pharmacokinetic properties led to the identification of compound **9m**, a potent, selective and orally bioavailable inhibitor of IGF-1R with in vivo efficacy in an IGF-driven mouse xenograft model.

Insulin-like growth factor 1 receptor (IGF-1R), a transmembrane receptor tyrosine kinase, has gained much attention in the field of cancer research and cancer drug discovery in recent years.[1–3] Accumulated preclinical research strongly suggests involvement of IGF-1R kinase activity and its signaling pathway in cell survival, proliferation, metastasis, and angiogenesis.[4–7] IGF-1R as a target for cancer therapy is being further validated in human clinical trials by both monoclonal antibodies directed against the receptor's extracellular ligand binding domain and small molecule IGF-1R directed tyrosine kinase inhibitors.[1,8]

Due to the importance of this target in oncogenesis, we have invested in a small molecule drug discovery platform which targets IGF-1R kinase activity. We have previously disclosed our efforts around novel 8-amino-imidazo[1,5-*a*]pyrazine- and 4-amino-imidazo[5,1-*f*][1,2,4]triazine-derived IGF-1R inhibitors including AQIP,[9] PQIP,[10] FQIT[11] as well as OSI-906,[12] the first and only selective small molecule dual IGF-1R/IR (insulin receptor) inhibitor currently in phase III clinical trials. These efforts focused on novel imidazopyrazine and imidazotriazine scaffolds substituted with two main pharmacophores: (1) a 2-phenylquinolin-7-yl moiety which binds to a hydrophobic back pocket of the enzyme, forming a critical H-bond to Lys1003 via the quinoline nitrogen or in the case of FQIT, via the quinoline nitrogen and the 8-F substituent; (2) a bridging cyclobutyl moiety which occupies the ribose binding pocket and acts as a linker to distal groups which access a solvent exposed region of the protein (Fig. 1). Efforts from both series concluded that substituents at the C3 position of the cyclobutyl moiety influenced both potency against IGF-1R and overall DMPK properties. Computer modeling suggested that larger ring systems, such as a cyclopentyl or cyclohexyl moiety should be tolerated as well in this ribose binding region. The 1,4-disubstituted cyclohexyl ring system was further prioritized among many designs since it positioned distal solvent exposed groups in a similar but slightly extended trajectory to that of the cyclobutyl linker. Herein we report medicinal chemistry efforts centered around the synthesis and optimization of a series of cyclohexyl substituted 8-amino-imidazo[1,5-*a*]pyrazine-derived inhibitors of IGF-1R, including the discovery of compound **9m** as a potent, selective, and orally bioavailable IGF-1R inhibitor with robust in vivo efficacy in an IGF-driven mouse xenograft model.

The general synthesis of C3 cyclohexyl substituted 8-amino-imidazo[1,5-*a*]pyrazines is shown in Scheme 1. The chloro-pyrazine **1** was coupled with activated ester **2** (readily available from *trans*-1,4-cyclohexanedicarboxylic acid monomethyl ester) to give amide **3** in good yield under mild conditions. Amide **3** was then treated with $POCl_3$ to form the imidazo[1,5-*a*]pyrazine scaffold,

* Corresponding authors. Fax: +1 631 845 5671.
E-mail address: mjin@osip.com (M. Jin).

0960-894X/$ - see front matter © 2010 Elsevier Ltd. All rights reserved.
doi:10.1016/j.bmcl.2010.12.094

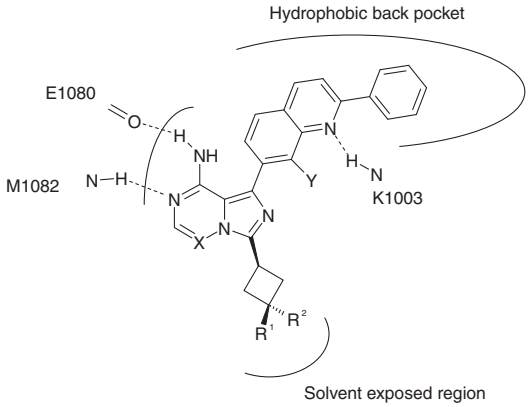

Compound	R^1	R^2	X	Y	IGF-1R cellular IC_{50} (nM)[a]
AQIP		H	CH	H	20
PQIP		H	CH	H	19
OSI-906	OH	Me	CH	H	24
FQIT	OH	Me	N	F	17

a. 3T3/huIGF-1R cells

Figure 1. Structures, IGF-1R potency, and key IGF-1R binding interactions of AQIP, PQIP, OSI-906, and FQIT.

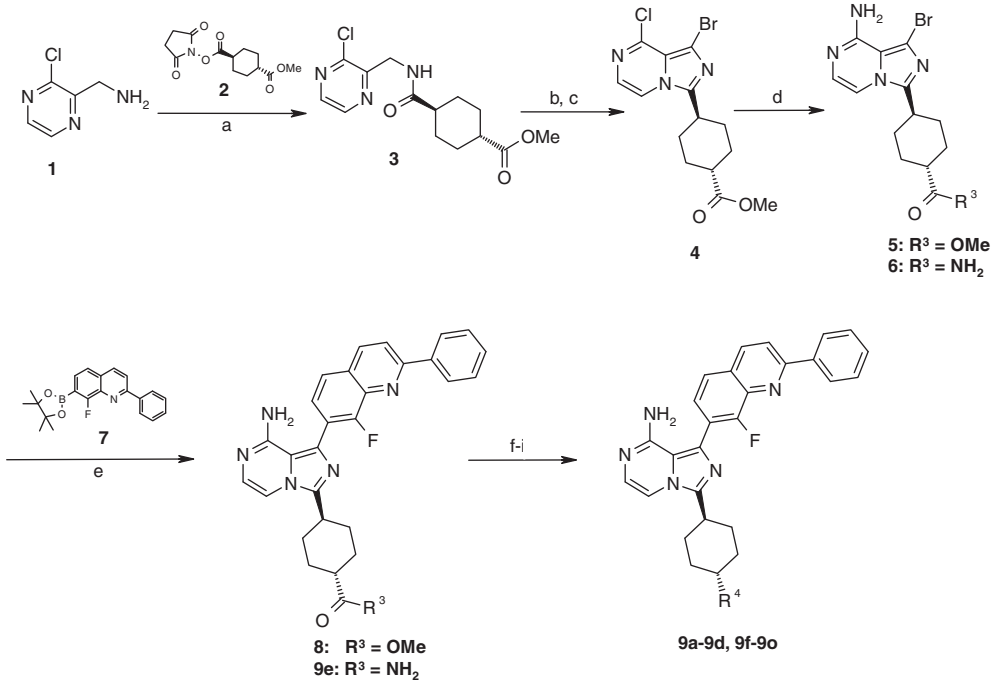

Scheme 1. Reagents and conditions: (a) 10% aq $NaHCO_3$, THF, rt, 88%; (b) $POCl_3$, DMF, MeCN, rt, 85%; (c) NBS, DMF, 0 °C, 91%; (d) NH_3, *i*PrOH, 90 °C, **5**: 70%, **6**: 15%; (e) $Pd(PPh_3)_4$, KF, dioxane–water (4:1, v/v), 90 °C, 65%; (f) to compound **9a** ($R^4 = CH_2OH$): **8**, LAH, THF, −78 °C, 70%; (g) to compound **9b** ($R^4 = CO_2H$): **8**, aq NaOH, EtOH, reflux, 95%; (h) to amides **9c–d**: **9b**, corresponding amine, TBTU, DIEA, DMF, 44–55%; (i) to compound **9f–9o**: **8**, corresponding amine, $AlMe_3$, toluene, 50 °C, 35–50%.

followed by *N*-bromosuccinimide (NBS) mediated bromination to give di-halogenated compound **4**. The ammonolysis of **4** afforded the desired 8-amino-product **5** along with amide **6** as a by-product. The key intermediate **8** was obtained from a subsequent Suzuki coupling of **5** with 8-fluoro-2-phenylquinoline boronate **7**.[13] Compound **8** proved to be a versatile intermediate and was used to synthesize primary alcohol **9a** by treatment with lithium aluminum hydride (LAH), carboxylic acid **9b** via treatment with aq NaOH in EtOH, and a cyclohexyl amide focused library. The focused amide library was synthesized via treatment of carboxylic acid **9b** with TBTU and either Me_2NH or $MeNH_2$ to provide analogs **9c** and **9d**, respectively. Primary amide **9e** was synthesized by direct coupling of intermediate **6** with quinoline boronate **7**. Alternatively, ester **8** was directly reacted with various aryl and heteroaryl amines in the presence of trimethylaluminum to give amides **9f**–**9o** in moderate yields.

The compounds synthesized in this series focused around the imidazopyrazine core which was substituted at the 1-position with the 8-fluoro-2-phenyl-quinolin-7-yl moiety discovered in the efforts leading to FQIT[11] and at the 3-position with a previously unexplored cyclohexyl linking moiety. The IGF-1R cell mechanistic potency of compounds **9a**–**9o** were determined in an ELISA-based assay utilizing 3T3/huIGF-1R cells, the results of which are summarized in Table 1. Primary alcohol **9a** displayed potent IGF-1R cellular activity. The carboxylic acid analog **9b** was significantly less potent, presumably due to its decreased cellular permeability, synonymous with such charged groups. Within the amido series, it appears that a proton donor (NH) was required, as evidenced by the potency loss of compound **9c** as compared to **9d** and **9e**. Furthermore, a variety of aryl and heteroaryl 5- or 6-monocyclic amides **9f**–**9h**, **9j**–**9l** were also highly potent IGF-1R inhibitors. Compound **9i** was ~4× less potent than several bioisosteric heteroarylamido analogs such as compound **9f** and **9g**. We speculate that the loss in potency may be a result of lower cellular permeability associated with the overall higher PSA as a result of inclusion of the triazole moiety. Additionally, a variety of 5,6-bicyclic amides were prepared from which benzimidazole **9m** (OSI-971) emerged as one of the more potent analogs.

Representative compounds from this series were progressed into pharmacokinetic studies in mice (Table 2). Compound **9a** displayed low oral bioavailability and low plasma exposure (low AUC and C_{max}), most likely due to extensive first pass metabolism as indicated by a high rate of clearance (more than double the mouse liver blood flow rate (~90 mL/min/kg)). Compound **9e**, when dosed orally, displayed modest exposure and bioavailability, speculated to be due to poor absorption as a result of low permeability as indicated by PAMPA. Compound **9f** was among one of the first representative compounds from the heteroaryl amido series profiled in mouse PK studies. Compound **9f** displayed very low bioavailability (5%), most likely due to both poor absorption and extensive metabolism. Acid **9b** was detected as a metabolite in plasma samples with slightly higher exposure than the parent compound. We hypothesized that gut metabolism may have contributed to this poor PK profile although we could not rule out the participation of first pass liver metabolism. We explored this hypothesis further by measuring the stability of **9f** in simulated intestinal fluid and after incubation over the course of a few hours, the acid metabolite **9b** was detected.[14] We then profiled acid **9b** in mouse PK studies and found that this compound was well absorbed and displayed good bioavailability. These results, when taken together, suggest that gut metabolism may be playing a role in limiting the bioavailability of compound **9f**. This prompted us to screen the remaining aryl and heteroaryl amides in simulated gastric fluid[15] and simulated intestinal fluid to evaluate their gut stability and rank compounds accordingly.[16] From these prescreening efforts, we determined that the benzimidazole amide **9m** was stable in the simulated gut stability assay as it did not produce any detectable level of acid **9b**. We were pleased that these results carried over in vivo as **9m** displayed high plasma exposures (high AUC and C_{max}) and good oral bioavailability in a subsequent mouse PK study, without any acid **9b** detected as a metabolite.

The favorable PK profile of **9m** prompted us to further evaluate this compound in subsequent in vivo studies. However, the synthetic route of this compound, shown in Scheme 1, was not ideal for scaling up to provide the multi-gram quantities of material required for in vivo studies due to moderate yields and tedious work up procedures in the $AlMe_3$ mediated coupling step. To resolve this issue, we developed an improved synthesis of **9m** as shown in Scheme 2. The intermediate **5** was hydrolyzed to give acid **10**, which was then coupled with 2-aminobenzimidazole using

Table 1
IGF-1R cellular potency of compounds **9a**–**9o**

Compound	R^4	IGF-1R cellular IC_{50}[a] (nM)
9a	CH_2OH	8
9b	CO_2H	285
9c	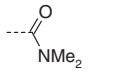	27
9d	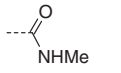	5
9e	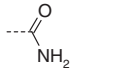	6
9f	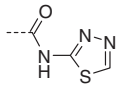	5
9g	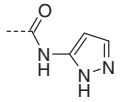	5
9h	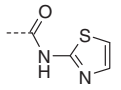	2
9i	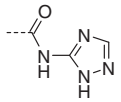	20
9j	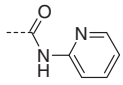	5
9k	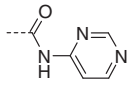	8
9l	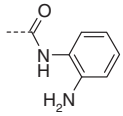	4
9m	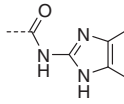	6
9n	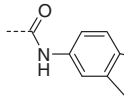	21
9o	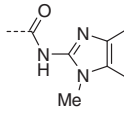	14

[a] 3T3/huIGF-1R cells.

Table 2
Key mouse PK parameters and PAMPA data of compounds **9a–b**, **9e**, **9f**, and **9m**

Compound	Mouse oral PK (25 mg/kg)			Mouse iv PK (5 mg/kg)		PAMPA (10^{-6} cm/s)	
	AUC (ng h/mL)	C_{max} (μM)	*F*%	V_{ss} (L/kg)	CL (mL/min/kg)	pH 5.0	pH 7.4
9a[a]	100	0.11	23	7	197	880	>1000
9b	7970	5.5	51	2.8	26	>1000	>1000
9e	3568	1.9	24	2.6	38	45	63
9f	297	0.13	5	3.2	73	73	86
9m	158,168	28	50	0.43	1	538	766

[a] 5 mg/kg oral dose, 2 mg/kg iv dose

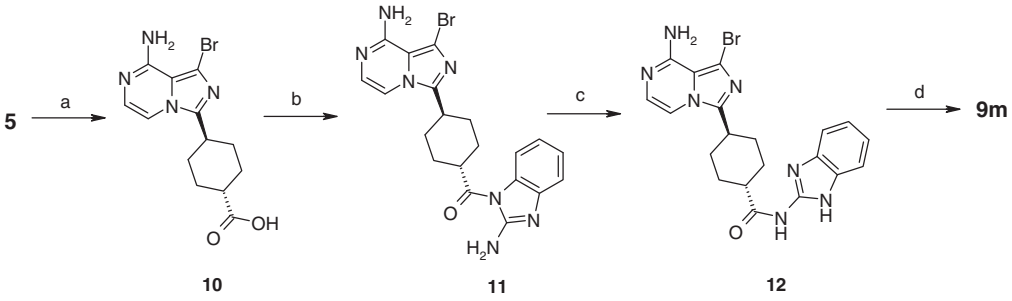

Scheme 2. Reagents and conditions: (a) 10 M aq NaOH, MeOH–water (3:1, v/v), 50 °C, 2 h, 95%; (b) 1.5 equiv 2-aminobenzimidazole, 1.5 equiv TFFH, DIEA, DMF, 0 °C, 1 h, 92%; (c) 0.5 equiv 2-aminobenzimidazole, DME, reflux overnight, 88%; (d) **7**, $Pd(PPh_3)_4$, KF, DME–water (4:1, v/v), 100 °C, overnight, 68%.

N,*N*,*N*′*N*′-tetramethylfluoroformamidinium hexafluorophosphate (TFFH)[17] as the coupling reagent to afford amide **11**. This amide was further converted to the desired regioisomer **12** by displacement with 0.5 equiv 2-aminobenzimidazole. It is noteworthy that all three reactions afforded clean conversions and the products from each step were isolated by simple filtrations. Finally, Suzuki coupling of amide **12** and boronate **7** provided **9m**. Using this newly developed synthesis, we successfully scaled up >100 g of material which was used in subsequent in vivo studies.

As shown in Figure 2, **9m** demonstrated dose dependent tumor growth inhibition (TGI) in the GEO human colon xenograft model.[18] The GEO model represents a naturally occurring IGF-driven tumor line and is sensitive to dual inhibition of IGF-1R and IR.[10] A 60 mg/kg daily oral dose of compound **9m** was very well tolerated and demonstrated significant tumor growth inhibition (98% TGI). At this dose, the blood glucose level was comparable to the control level (Fig. 2b).

To determine its kinase selectivity, **9m** was screened against a panel of 90 kinases using a Caliper EZ Reader mobility shift assay and only showed significant activity (>50% inhibition at 1 μM concn) against the IGF-1 and Insulin receptors. Preclinical safety screens of **9m** against a broad range of 68 enzymes, receptors, and ion channels at 10 μM concentration did not reveal any significant off-target activities. Thus **9m** is a highly selective dual IGF-1R and IR inhibitor. Furthermore, **9m** is not genotoxic (Ames negative ± S9 fractions) and does not significantly inhibit any major CYP isoforms (Table 3).

In summary, structural modifications at the C3 position of an imidazopyrazine-derived series of IGF-1R inhibitors led to the discovery of a series of C3-substituted cyclohexyl-based inhibitors.

Table 3
CYP inhibition of **9m**

CYP inhibition	IC_{50} (μM)
3A4	>20
1A2	>20
2C9	9.8
2C19	>20
2D6	>20

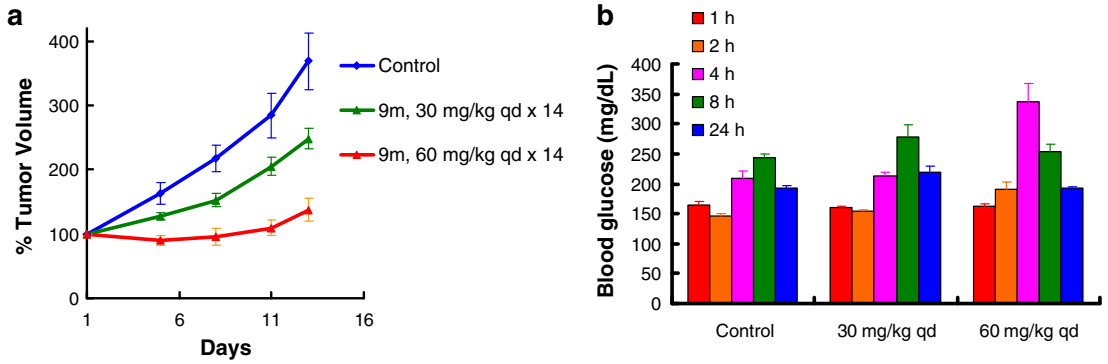

Figure 2. (a) Dose-dependent efficacy of **9m** in a GEO xenograft model. Plotted data are mean tumor volumes expressed as a percentage on initial volume ± SE. Compound **9m** was dosed once daily (qd) for 14 days. (b) Non-fasted blood glucose at indicated times in GEO tumor bearing animals following 14 days of dosing with **9m**. Data shown are mean of $n = 3$ at each time point.

Optimization of potency, drug metabolism and pharmacokinetic properties led to a series of cyclohexyl-based aryl and heteroaryl amides as the preferred moiety and ultimately to the discovery of compound **9m**, a potent, selective, and orally bioavailable IGF-1R inhibitor with robust in vivo efficacy in an IGF-driven mouse xenograft model.

Acknowledgments

The authors gratefully acknowledge Dr. Yingjie Li and Ms. Viorica M. Lazarescu for analytical support, and Mr. Paul Maresca, Mr. Pete Meyn, Mr. Roy Turton and the Leads Discovery Group for conducting in vitro ADMET studies.

References and notes

1. Li, R.; Pourpak, A.; Morris, S. W. *J. Med. Chem.* **2009**, *52*, 4981.
2. Adams, T. E.; Epa, V. C.; Garrett, T. P.; Ward, C. W. *Cell. Mol. Life Sci.* **2000**, *57*, 1050.
3. De Meyts, P.; Whittaker, J. *Nat. Rev. Drug Disc.* **2002**, *1*, 769.
4. Buck, E.; Eyzaguirre, A.; Rosenfeld-Franklin, M.; Thomson, S.; Mulvihill, M.; Barr, S.; Brown, E.; O'Connor, M.; Yao, Y.; Pachter, J.; Miglarese, M.; Epstein, D.; Iwata, K.; Haley, J.; Gibson, N.; Ji, Q. *Cancer Res.* **2008**, *68*, 8322.
5. Garcia-Echeverria, C.; Pearson, M. A.; Marti, A.; Meyer, T.; Mestan, J.; Zimmermann, J.; Gao, J.; Brueggen, J.; Capraro, H.; Cozens, R.; Evans, D.; Fabbro, D.; Furet, P.; Porta, D.; Liebetanz, J.; Martiny-Baron, G.; Ruetz, S.; Hofmann, F. *Cancer Cell* **2004**, *5*, 231.
6. LeRoith, D.; Roberts, C. T., Jr. *Cancer Lett.* **2003**, *195*, 127.
7. Pollak, M. *Nat. Rev. Cancer* **2008**, *8*, 915.
8. Osborne, R. *Nat. Biotechnol.* **2008**, *26*, 719.
9. Mulvihill, M.; Ji, Q.; Coate, H.; Cooke, A.; Dong, H.; Feng, L.; Foreman, K.; Rosenfeld-Franklin, M.; Honda, A.; Mak, G.; Mulvihill, K.; Nigro, A.; O'Connor, M.; Pirrit, C.; Steinig, A.; Siu, K.; Stolz, K.; Sun, Y.; Tavares, P.; Yao, Y.; Gibson, N. *Bioorg. Med. Chem.* **2008**, *16*, 1359.
10. Ji, Q.; Mulvihill, M.; Rosenfeld-Franklin, M.; Cooke, A.; Feng, L.; Mak, G.; O'Connor, M.; Yao, Y.; Pirritt, C.; Buck, E.; Eyzaguirre, A.; Arnold, L.; Gibson, N.; Pachter, J. A. *Mol. Cancer Ther.* **2007**, *6*, 2158.
11. Jin, M.; Gokhale, P.; Cooke, A.; Foreman, K.; Buck, E.; May, E.; Feng, L.; Bittner, M.; Kadalbajoo, M.; Landfair, D.; Siu, K.; Stolz, K.; Werner, D.; Laufer, R.; Li, A.; Dong, H.; Steinig, A.; Kleinberg, A.; Yao, Y.; Pachter, J.; Wild, R.; Mulvihill, M. J. *ACS Med. Chem. Lett.* **2010**, *1*, 510. Compound **9b** in this manuscript is referred to FQIT (*cis*-3-[4-amino-5-(8-fluoro-2-phenyl-quinolin-7-yl)-imidazo[5,1-*f*][1,2,4]triazin-7-yl]-1-methyl-cyclobutanol) herein.
12. Mulvihill, M.; Cooke, A.; Rosenfeld-Franklin, M.; Buck, E.; Foreman, K.; Landfair, D.; O'Connor, M.; Pirrit, C.; Sun, Y.; Yao, Y.; Arnold, L.; Gibson, N.; Ji, Q. *Future Med. Chem.* **2009**, *1*, 1153.
13. Arnold, L. D.; Cesario, C.; Coate, H.; Crew, A. P.; Dong, H.; Foreman, K.; Honda, A.; Laufer, R.; Li, A. H.; Mulvihill, K. M.; Mulvihill, M. J.; Nigro, A.; Panicker, B.; Steinig, A. G.; Sun, Y.; Weng, Q.; Werner, D. S.; Wyle, M. J.; Zhang, T. WO 2005097800A1, 2005.
14. Simulated intestinal fluids: Phosphate buffer (pH 6.8) + pancreatin (10 mg/mL).
15. Simulated gastric fluids: Hydrochloric acid (0.1 M) + sodium chloride (2 mg/mL) + pepsin (3.2 mg/mL).
16. Simulated gastric fluids and intestinal fluids (1 mL) were equilibrated at 37 °C in a 24-well plate, and individually spiked with solutions of compounds **9f–9o** in DMSO (1 μL) to give concentrations of approximately 2 μM. The bulk samples were held at 37 °C on an orbital shaker, and aliquots of 100 μL were removed immediately after spiking, and at five subsequent time points up to approximately 5 h. These samples underwent the normal analytical procedure for these compounds, consisting of protein precipitation with chilled methanol (−20 °C) followed by HPLC–MS/MS.
17. Carpino, L. A.; El-Faham, A. *J. Am. Chem. Soc.* **1995**, *117*, 5401.
18. Female *nu*/*nu* CD-1 mice were used for xenograft studies. To assess anti-tumor efficacy, cells were implanted sc in the right flank. Tumors were allowed to establish to 200 ± 50 mm^3 before randomization into treatment groups. Tumor volumes were determined twice weekly from caliper measurements by $V = (\text{length} \times \text{width}^2)/2$. Tumor growth inhibition (TGI) was determined by $\%TGI = \{1 - [(T_t/T_0)/(C_t/C_0)]/1 - [C_0/C_t]\} \times 100$, where T_t = tumor volume of treated animal x at time t, T_0 = tumor volume of treated animal x at time 0, C_t = median tumor volume of control group at time t, and C_0 = median tumor volume of control group at time 0. Mean %TGI was calculated for the entire dosing period for each group. Significant anti-tumor activity is defined as mean %TGI >50%.